Multimodal nonlinear spectral microscopy based on a femtosecond Cr:forsterite laser

Shi-Wei Chu, I-Hsiu Chen, Tzu-Ming Liu, Ping Chin Chen,* and Chi-Kuang Sun

Department of Electrical Engineering and Graduate Institute of Electro-Optical Engineering, National Taiwan University, Taipei 10617, Taiwan

Bai-Ling Lin

Institute of Molecular Biology, Academia Sinica, Taipei 11529, and Molecular and Cell Biology Division, Development Center for Biotechnology, Taipei 10659, Taiwan

Received May 9, 2001

We demonstrate a novel multimodal nonlinear spectral microscopy based on a femtosecond Cr:forsterite laser at 1230 nm. By acquiring the whole nonlinear spectrum in the visible and near-NIR region, this novel technique allows a combination of different imaging modalities, including second-harmonic generation, third-harmonic generation, and multiple-photon fluorescence. Combined with the selected excitation wavelength, which is located in the IR transparency window, this microscopic technique can provide high penetration depth with reduced damage and is ideal for studying living cells.

OCIS codes: 180.1790, 190.7110.

Laser scanning fluorescence microscopy[1] has made a major effect on life sciences in recent years with the development of special imaging modalities. The use of near-IR (NIR) light, generally near 800 nm, in two-photon fluorescence (2PF) microscopy leads to deeper penetration in most biological specimens. Even with less photodamage than with single-photon microscopy, this widely accepted 2PF microscopy technique still requires in-focus nonlinear absorption.[1] The in-focus photodamage[2] and the common issues of limited dye penetration and toxicity indicate the importance of finding alternative spectral ranges and imaging modalities. It is also desirable to take advantage of all available intrinsic biological signals provided through different nonlinearities such as harmonic generation. According to previous studies, light attenuation (including both absorption and scattering) in most biological specimens[3,4] reaches a minimum near the 1300-nm wavelength. Previous studies comparing penetration depths of 800- and 1300-nm light sources for optical coherent tomography in live tissues suggested superior performance at 1300 nm.[5] Moving the operating wavelength of a nonlinear microscope to 1200–1300 nm can not only increase the penetration depth in most biological tissues but also reduce the multiple-photon absorption cross section[6] and thus reduce potential photodamage. Moreover, moving the operating wavelength makes third-harmonic generation (THG) microscopy possible because the use of the visible THG wavelength allows one to avoid the strong UV absorption of protein. A laser wavelength in this optimal penetration window not only opens up the possibility of different imaging modalities, including THG, second-harmonic generation (SHG), three-photon fluorescence (3PF), and 2PF, but also opens the whole visible and NIR region for efficient nonlinear spectral detection while the pump is away from the sensitivity range of silicon detectors.

In this Letter we demonstrate a technique for multimodal nonlinear spectral microscopy based on the use of a femtosecond Cr:forsterite laser at 1230 nm.[7] The laser output was focused into samples with a high-numeral-aperture objective. A photoexcited nonlinear spectrum was collected with an opposing objective and then directed into a CCD-based spectrometer. We filtered out the fundamental IR beam with a glass filter. Mechanical stages were used to achieve a raster scan for $x-y-z-\lambda$ images, with a nonlinear spectrum corresponding to each pixel recorded. The pixel-acquisition time ranges from 0.02 to 0.5 s, which can be improved by incorporation of a beam-scanning system.

Figure 1 shows the emission spectra from the cell wall of the ground tissue in *Zea mays* stem with a 0.45-mW, 365-nm UV light (dotted curve), 50-mW, 780-nm Ti:sapphire laser (120-fs pulse width; dashed curve); and a 150-mW, 1230-nm Cr:forsterite laser (solid curve). Broad autofluorescence covering the whole visible and NIR region can be observed with both UV (single-photon fluorescence) and Ti:sapphire excitation (2PF), whereas, with 1230-nm excitation,

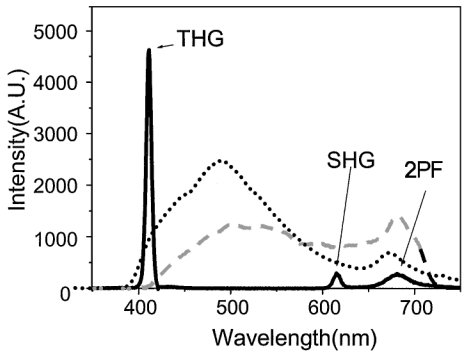

Fig. 1. Nonlinear emission spectra from the cell wall of ground tissue in maize stem with three different sources: UV light (dotted curve), a Ti:sapphire laser (dashed curve), and a Cr:forsterite laser (solid curve). TPA, two-photon absorption.

0146-9592/01/231909-03$15.00/0

only weak residue 2PF (680 nm) can be observed. With suppressed background autofluorescence by use of 1230-nm excitation, the whole visible and NIR region can then be left for efficient multiple-photon fluorescence dye to label different functional molecules. Our previous studies with a 1230-nm Cr:forsterite laser indicated efficient 2PF and 3PF in common bioprobes.[7]

It is interesting to notice the symmetric SHG and THG spectra centered at 615 and 410 nm, respectively, with intensities stronger than 2PF in the Cr:forsterite excited spectrum. Unlike in single- and multiple-photon fluorescence processes, only virtual states are involved in harmonic generation that results in no energy deposition, and thus no photodamage or bleaching is expected. Since SHG does not occur in optically isotropic media, SHG microscopy was demonstrated in the studies of SHG crystals[8] and was then applied to biological study, including study of membrane potentials[9,10] and tissue polarity.[11] THG microscopy was applied in transparent objects,[12,13] and effective THG occurred only in interfaces with optical inhomogeneity.[12] With a cubic dependence, the THG process provides even better intrinsic sectioning resolution than SHG with the same excitation laser wavelength but experiences stronger signal attenuation with depth.

Figure 2 shows specific $x-y-\lambda$ images corresponding to THG, SHG, and 2PF in ground tissue in maize stem taken at a depth of 60 μm from the sample surface. The sample thickness was ~500 μm. With an average power of 100 mW before the sample and a focused spot size of 1.3 μm, the intensity at the focus is $9-50 \times 10^{10}$ W/cm^2, depending on the focal depth inside the sample. THG shows the longitudinal cell walls in the center of the image and the transverse cell walls of several adjacent cells, revealing the ability of THG to pick up the whole cell profile [Figs. 2(F) and 2(G)]. SHG shows mainly the longitudinal walls, and 2PF indicates the distribution of the autofluorescent molecules. More than 500-μm penetration depth in the maize stem sample can be achieved with a Cr:forsterite laser. Figure 2(E) shows a sectional image taken at 420-μm depth from the same sample. Since the maize stems have an attenuation coefficient of 34 cm^{-1} at 1230 nm. The 360-μm depth difference thus corresponds to an illumination intensity attenuation of 3.4, with a 2PF–SHG attenuation of 11.5 and a THG attenuation of 39. With the same signal integration time, we amplified the SHG–2PF signal intensity by 11.5 times and the THG signal intensity by 39 times in Fig. 2(E) to compare with Fig. 2(D). Similar image quality and brightness can be obtained for both figures, indicating good agreement between our penetration capability and previous linear attenuation measurements.

It is also interesting to notice that THG and SHG do not occur in the same position. According to a previous study,[12] interface-sensitive THG provides cell-wall images. Regarding SHG, we believe that it comes mainly from specially organized nanostructures, such as crystalline microfibrils on the secondary walls of plant cells, breaking three-dimensional optical centrosymmetry. The strength of the SHG signals can vary according to the orientation of the crystalline structures, which may have different $\chi^{(2)}$ matrix components. This mechanism provides an opportunity for structural orientation studies in which SHG with controlled illumination polarization is used. For instance, by variation of the incident-light polarization (as in Fig. 3), the concentric silica deposition in the dumbbell-shaped silica cells of rice leaf produces SHG images with a particular orientation with respect to that of the illumination polarization. In contrast, no polarization dependence was found in the THG images. Along with mineral deposition in plant cells,

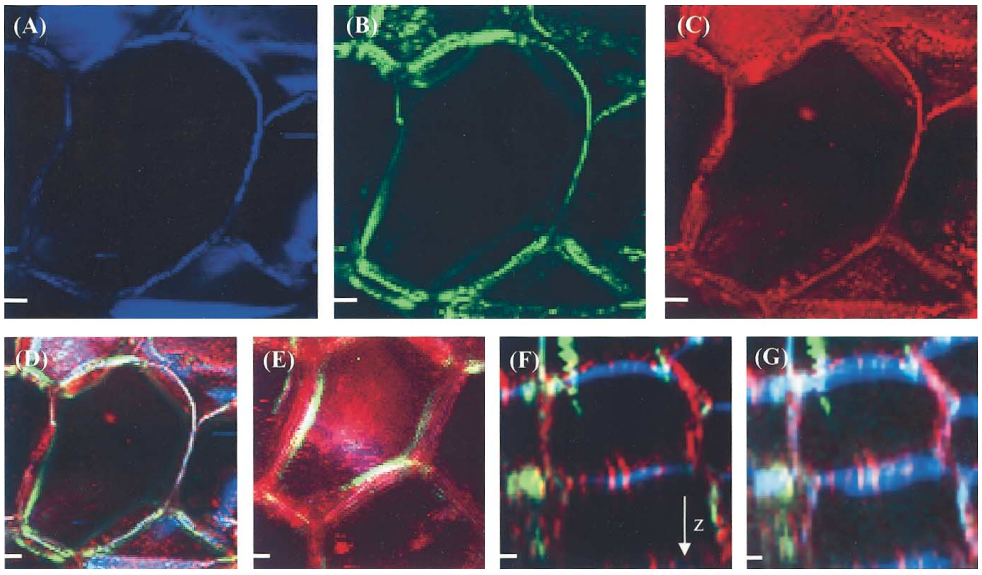

Fig. 2. Cross-sectional $x-y-\lambda$ maize stem images corresponding to (A) THG, (B) SHG, and (C) 2PF. (D) Combined image taken at 60 μm from the sample surface. THG, SHG, and 2PF signals are denoted by blue, green, and red, respectively. (E) Combined $x-y-\lambda$ image taken at 420 μm from the sample surface. (F), (G) $x-z-\lambda$ images of ground tissue cells with regular and log scales, respectively. Scale bars, 15 μm.

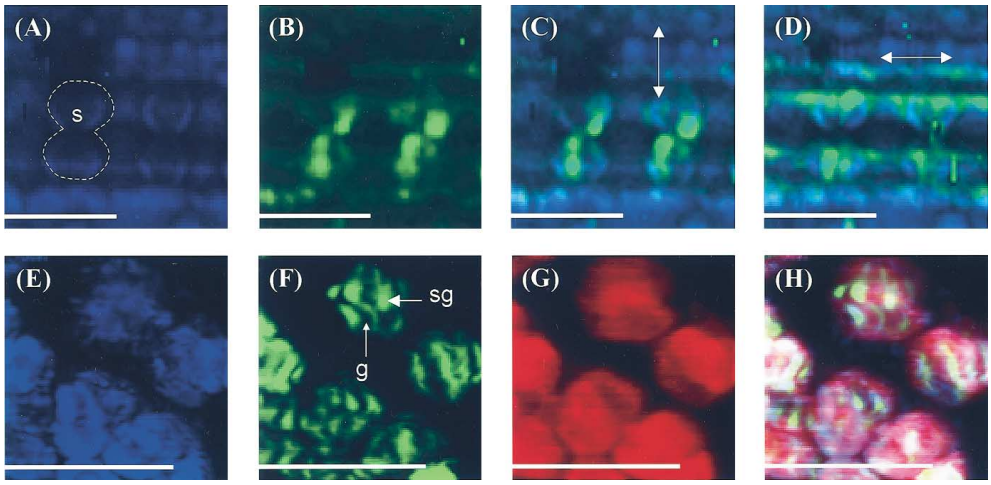

Fig. 3. (A) THG, (B) SHG, and (C) combined multimodal $x-y-\lambda$ images taken from adaxial surface of rice leaf in region with silica cells (dotted curve). No 2PF was observed. (D) Multimodal $x-y-\lambda$ images corresponding to different incident polarizations (shown as arrows). (E), (F), (G), and (H) show THG, SHG, 2PF, and combined multimodal $x-y-\lambda$ images, respectively, of chloroplasts inside a live mesophyll cell of *Commelina communis* L. s, silica cell, g, grana; sg, starch granule. Scale bars, 15 μm.

laminated membrane structures are also potential candidates for producing strong SHG activity. In chloroplasts, in addition to the TPF signals generated from the highly autofluorescing photosynthetic pigments, THG and SHG appear in different suborganelle compartments [Figs. 3(D)–3(H)]. Matching Fig. 3(F) with TEM images of similar specimens, we concluded that the signals of SHG are the result of orderly stacked thylakoid membranes in grana and the highly structured starch granules in the chloroplasts, whereas THG provides information on suborganellar interfaces. Our study indicates that, with interface- and structure-sensitive THG and SHG signals, we can reduce photodamage and photobleaching to a minimum level and avoid dye penetration and toxicity in live cells by labeling their subcellular structures with intrinsic harmonic-generation signals.

In summary, we have demonstrarted a multimodal nonlinear spectral microscopy based on a femtosecond Cr:forsterite laser. With illumination on the lowest attenuation position of most living biological specimens, the use of a Cr:forsterite laser provides high penetration capability. Moreover, moving the excitation wavelength to the 1200–1300-nm region makes simultaneous SHG–THG microscopy possible because of a visible SHG–THG wavelength that can avoid strong UV absorption of protein. By acquisition of the whole nonlinear spectrum in the visible and NIR region, this novel microscopic technique allows a combination of different imaging modalities, including SHG, THG, 2PF, and 3PF. Although multiphoton fluorescence provides information on functional molecules, SHG and THG provide images of specially organized biological subcellular nanostructures and biological interfaces. Unlike single-photon and multiphoton absorption, harmonic generation involves only the virtual state without energy deposition, thus causing no photodamage or bleaching, and is ideal for studying living cells.

This work was sponsored by National Science Center of Taiwan through grants 90-2215-E-002-039, 90-2911-I-002-011, and 89-2311-B-001-137. C.-K. Sun's e-mail address is sun@cc.ee.ntu.edu.tw.

*Permanent address: Department of Electrical Engineering, State University of New York at Buffalo, Buffalo, New York 14260-2050.

References

1. W. Denk, J. H. Strickler, and W. W. Webb, Science **248,** 73 (1990).
2. K. König, P. T. C. So, W. W. Mantulin, and E. Gratton, Opt. Lett. **22,** 135 (1997).
3. P. C. Cheng, S. J. Pan, A. Shih, K.-S. Kim, W. S. Liou, and M. S. Park, J. Microsc. **189,** 199 (1998).
4. R. R. Anderson and J. A. Parish, J. Invest. Dermatol. **77,** 13 (1981).
5. B. E. Bouma, G. J. Tearney, I. P. Bilinsky, B. Golubovic, and J. G. Fujimoto, Opt. Lett. **21,** 1839 (1996).
6. I.-H. Chen, S.-W. Chu, C.-K. Sun, P. C. Cheng, and B.-L. Lin, "Wavelength dependent damage in biological multi-photon confocal microscopy: a micro-spectroscopic comparison between femtosecond Ti:sapphire and Cr:forsterite laser sources," Opt. Quantum Electron. (to be published).
7. T.-M. Liu, S.-W. Chu, C.-K. Sun, B.-L. Lin, P. C. Cheng, and I. Johnson, Scanning **23,** 249 (2001).
8. J. N. Gannaway and C. J. R. Sheppard, Opt. Quantum Electron. **10,** 435 (1978).
9. L. Moreaux, O. Sandre, M. Blanchard-Desce, and J. Mertz, Opt. Lett. **25,** 320 (2000).
10. G. Peleg, A. Lewis, M. Linial, and L. M. Loew, Proc. Natl. Acad. Sci. USA **96,** 6700 (1999).
11. I. Freund, M. Deutsch, and A. Sprecher, Biophys. J. **50,** 693 (1986).
12. D. Yelin and Y. Silberberg, Opt. Express **5,** 169 (1999), http://www.opticsexpress.org.
13. M. Muller, J. Squier, K. R. Wilson, and G. J. Brakenhoff, J. Microsc. **191,** 266 (1998).